ARMY RESEARCH LABORATORY

Viscous Hydrodynamic Model of Non-linear Plasma Oscillations in Two-Dimensional Gated Conduction Channels and Application to the Detection of Terahertz Signals

by Sergey Rudin

ARL-TR-5157 **April 2010**

Approved for public release; distribution unlimited.

NOTICES

Disclaimers

The findings in this report are not to be construed as an official Department of the Army position unless so designated by other authorized documents.

Citation of manufacturer's or trade names does not constitute an official endorsement or approval of the use thereof.

Destroy this report when it is no longer needed. Do not return it to the originator.

Army Research Laboratory
Adelphi, MD 20783-1197

ARL-TR-5157 **April 2010**

Viscous Hydrodynamic Model of Non-linear Plasma Oscillations in Two-Dimensional Gated Conduction Channels and Application to the Detection of Terahertz Signals

Sergey Rudin
Sensors and Electron Devices Directorate, ARL

Approved for public release; distribution unlimited.

REPORT DOCUMENTATION PAGE

Form Approved
OMB No. 0704-0188

Public reporting burden for this collection of information is estimated to average 1 hour per response, including the time for reviewing instructions, searching existing data sources, gathering and maintaining the data needed, and completing and reviewing the collection information. Send comments regarding this burden estimate or any other aspect of this collection of information, including suggestions for reducing the burden, to Department of Defense, Washington Headquarters Services, Directorate for Information Operations and Reports (0704-0188), 1215 Jefferson Davis Highway, Suite 1204, Arlington, VA 22202-4302. Respondents should be aware that notwithstanding any other provision of law, no person shall be subject to any penalty for failing to comply with a collection of information if it does not display a currently valid OMB control number.
PLEASE DO NOT RETURN YOUR FORM TO THE ABOVE ADDRESS.

1. REPORT DATE *(DD-MM-YYYY)*	2. REPORT TYPE	3. DATES COVERED (From - To)
April 2010	Final	October 2009 to April 2010

4. TITLE AND SUBTITLE
Viscous Hydrodynamic Model of Non-linear Plasma Oscillations in Two-Dimensional Gated Conduction Channels and Application to the Detection of Terahertz Signals

5a. CONTRACT NUMBER

5b. GRANT NUMBER

5c. PROGRAM ELEMENT NUMBER

6. AUTHOR(S)
Sergey Rudin

5d. PROJECT NUMBER

5e. TASK NUMBER

5f. WORK UNIT NUMBER

7. PERFORMING ORGANIZATION NAME(S) AND ADDRESS(ES)
U.S. Army Research Laboratory
ATTN: RDRL-SEE-M
2800 Powder Mill Road
Adelphi, MD 20783-1197

8. PERFORMING ORGANIZATION REPORT NUMBER
ARL-TR-5157

9. SPONSORING/MONITORING AGENCY NAME(S) AND ADDRESS(ES)

10. SPONSOR/MONITOR'S ACRONYM(S)

11. SPONSOR/MONITOR'S REPORT NUMBER(S)

12. DISTRIBUTION/AVAILABILITY STATEMENT
Approved for public release; distribution unlimited.

13. SUPPLEMENTARY NOTES

14. ABSTRACT
The conduction channel of a heterostructure High Electron Mobility Transistor can act as a plasma wave resonator for charge density oscillations at frequencies significantly higher than the transistor cut-off frequency in a short channel device. In the Dyakonov-Shur detector a short channel HEMT is used for the resonant tunable detection of electromagnetic radiation in the low terahertz range. Here I evaluated the resonant nonlinear response and obtained the temperature dependence of the quality factor of the plasma resonance. I find that in high mobility gated semiconductor conduction channels the quality of the resonance is limited by the temperature dependent viscosity of the electron fluid.

15. SUBJECT TERMS
Terahertz detector, plasma resonance

16. SECURITY CLASSIFICATION OF:			17. LIMITATION OF ABSTRACT	18. NUMBER OF PAGES	19a. NAME OF RESPONSIBLE PERSON
a. REPORT	b. ABSTRACT	c. THIS PAGE			Sergey Rudin
Unclassified	Unclassified	Unclassified	UU	36	19b. TELEPHONE NUMBER (*Include area code*) (301) 394-0206

Standard Form 298 (Rev. 8/98)
Prescribed by ANSI Std. Z39.18

Contents

List of Figures iv

Acknowledgment v

1. Summary 1

2. Introduction 1

3. Quasi-classical Approximation 4

4. Electron-electron Scattering Rate and Mean Free Path in Two-dimensional Gated Channels 7

5. Derivation of the Hydrodynamic Equations and the Transport Coefficients 9

6. Nonlinear Response of the Channel Confined Electron Plasma to a Time-harmonic Signal 15

7. Conclusions 24

8. References 26

Distribution List 28

List of Figures

Figure 1. Schematic structure of a conduction channel in a FET. The gate length L is much larger than the mean free path of electron-electron collisions λ_{ee} but smaller than the mean free path of electron-phonon and electron-impurity scattering. 2

Figure 2. Schematic geometry of FET operating in detector mode for (a) induced ac voltage and (b) induced ac current.....3

Figure 3. The electron mean free path λ_{ee} determined by the electron-electron scattering is shown as a function of temperature for the GaAs channel, when the gate voltage above the threshold value is $U_0 = 0.5$ V. 9

Figure 4. Coefficients of kinematic viscosity (left panel) and thermal conductivity divided by density (right panel) are shown as functions of temperature for the (a) GaAs and (b) GaN channels.....14

Figure 5. Response function of the GaAs channel based detector at two different temperatures: $T/T_F = 0.1$ (solid line) and $T/T_F = 0.15$ (broken line). 19

Figure 6. Response function in the case of strongly damped plasma oscillations, giving a broadband detector response, for two different values of friction parameter, $\tau s_0/L = 0.3$ and 0.2 with $\nu/s_0L = 0.001$. 19

Figure 7. An example of electron temperature distribution in the conduction channel with $s_0\tau/L = 2$, at two different times, (a) $ts_0/L = 1$ and (b) $ts_0/L = 2$. Both distributions are evaluated at the resonance frequency ω_0, with the amplitude of the applied signal equal to $0.1U_0$. 21

Figure 8. Electron temperature distribution in the GaAs conduction channel at $T_0 = 0.1T_F$ at two different times, (a) $ts_0/L = 1$ and (b) $ts_0/L = 2$. Both distributions are evaluated at the resonance frequency ω_0, with the amplitude of the applied signal equal to $0.01U_0$. 21

Figure 9. Plasma resonator quality factor is shown as function of temperature for (a) GaAs and (b) GaN channels with length L = 0.5 μm. The resonance is at $f_0 \sim 0.5$ THz.....23

Figure 10. Plasma resonator quality factor is shown as function of temperature for a GaAs detector with channel length L = 180 μm. The resonance is at $f_0 \sim 1.2$ GHz. 24

Acknowledgment

I thank Frank Crowne for helpful discussions.

INTENTIONALLY LEFT BLANK.

1. Summary

This report details my study of the non-linear plasma oscillations in a semiconductor conduction channel controlled by a gate. The analysis is based on the hydrodynamic equations derived from the Boltzmann equation for a parabolic conduction band. The hydrodynamic approximation derived here includes the effects of viscosity, finite mobility, and temperature gradients in the channel. I evaluated the electron-electron collision limited mean free path as a function of temperature and gate potential. When this path is much smaller than the wavelength of the density variations, the electron gas in the channel can be treated as a two-dimensional fluid. The flow is described by the Navier-Stokes equation and the heat conduction equation. The quality of the plasma resonance is limited by the electron mobility and the viscosity of the electron fluid. Using the relaxation time approximation I evaluated the hydrodynamic transport coefficients, and showed that at low temperatures in high mobility channels the quality factor of the plasma resonance is limited by the viscosity. The hydrodynamic nonlinearities in the gated channel subjected to a time-harmonic signal, induce a constant drain-to-source voltage with a resonant dependence on the frequency. This effect can be used for the detection of electromagnetic radiation by the Dyakonov-Shur detector. I evaluated the detector response for particular dimensions and values of mobility at which plasma resonances are in the terahertz range. I also evaluated the quality of the plasma resonance as a function of temperature, and showed how the viscosity effects limit the quality factor at low temperatures.

2. Introduction

The conduction channel of a semiconductor Field Effect Transistor (FET) or a heterostructure High Electron Mobility Transistor (HEMT) can act as a plasma wave resonator for density oscillations in quasi-two-dimensional (2D) electron gas. The plasma wave here refers to electron density excitation, possible at frequencies significantly higher than the FET cut-off frequency in a short channel device. The hydrodynamic model predicts a resonance response to electromagnetic radiation at the plasma oscillation frequency which can be used for detection, mixing, and frequency multiplication in the terahertz range (*1, 2*). In particular, the hydrodynamic nonlinearities produce a constant source-to-drain voltage when gate-to-channel voltage has a time-harmonic component. In the Dyakonov-Shur detector, a short channel HEMT is used for the resonant tunable detection of terahertz radiation. The non-linear plasma response has been observed in InGaAs (*3, 4*) and GaN (*5–8*) HEMTs, in the frequency range from 0.2 to 2.5 THz. The emission of radiation is also possible due to amplification of plasma oscillations upon reflection of plasma waves at the channel lateral boundaries, which has been shown to lead to plasma instability under certain boundary conditions (*9*). For recent reviews of the

experimental efforts in detection and emission of THz radiation by using such submicron channels see references 7 and 9. The results show that short channel FETs can be used both for tunable resonant and broadband detection of electromagnetic radiation in THz and sub-THz range. In addition, a resonant frequency response was also studied in a few GHz range using a 180 μm long channel GaAs HEMT (*10*).

The plasma waves in the gated two-dimensional channels have linear dispersion law (*1*)

$$\omega_{pl}(q) = sq = q\sqrt{\frac{e\left(U_g - U_{th}\right)}{m}}, \tag{1}$$

where s is the plasma wave velocity, q is the in-plane wave vector, e is the electron charge, U_g is the gate voltage, U_{th} is the threshold voltage for the formation of the conduction channel, and m is the effective electron mass. For example, if gate voltage is 1 V above the threshold, the plasma wave velocity in GaAs and GaN channels s ~ 10^8cm/s, usually much higher than the electron drift velocity. Note that the dispersion law in the gated channel is different from the dispersion law in the un-gated two-dimensional electron gas (ungated parts of FET) with sheet density n_0, $\omega(q) = (qe^2n_0/2m)^{1/2}$.

In a FET channel with length L, figure 1, the eigen-frequencies of the plasma standing waves are odd multiples of the fundamental plasma frequency, given by

$$\omega_0 = \frac{\pi}{2L}\sqrt{\frac{e\left(U_g - U_{th}\right)}{m}}. \tag{2}$$

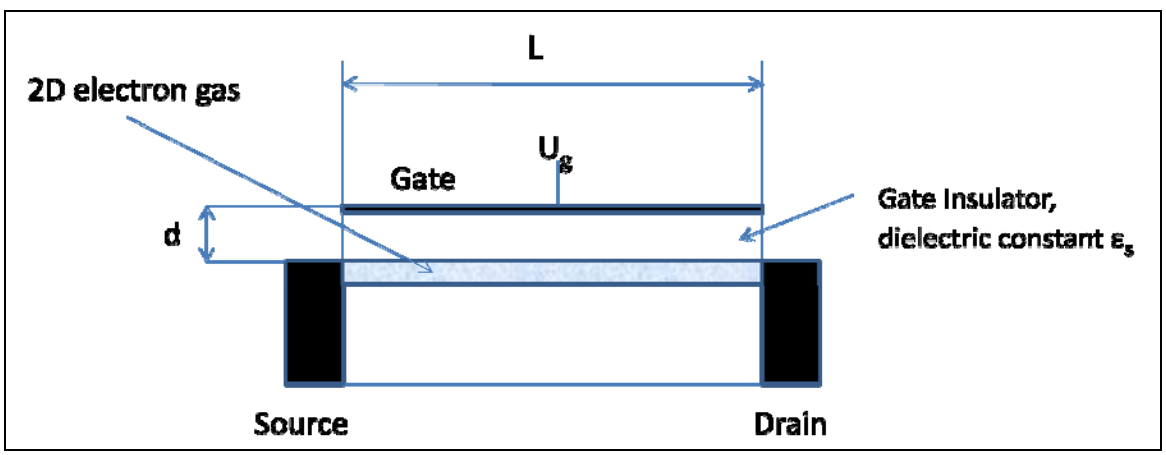

Figure 1. Schematic structure of a conduction channel in a FET. The gate length L is much larger than the mean free path of electron-electron collisions λ_{ee} but smaller than the mean free path of electron-phonon and electron-impurity scattering.

If the mean free path of electron-electron collisions λ_{ee} is much smaller than the channel length L, the plasma transport in the channel can be studied within the hydrodynamic model of the electron density waves. If the momentum relaxation time τ_p, determined by electron-phonon and

electron-impurity collisions is such that $\omega_0\tau_p >> 1$, the FET can operate as a resonant detector tunable by the gate voltage. If $\omega_0\tau_p < 1$, the detector response will be broadband. The wavelength of the incoming electromagnetic radiation in the terahertz range is much larger than the device dimensions, and the original proposal of the Dyakonov-Shur detector in reference 1 included an antenna structure in order to collect the radiation. In a design with a slot antenna, an ac voltage U_{ac} is induced between source and gate contacts as shown in figure 2(a). In a design with a bow tie antenna, an ac current I_{ac} is induced between source and gate, figure 2(b). In the resent realizations of the HEMT based detector, references 3–7, the metal pads of the electrodes perform the role of the antenna. The gate voltage U_g is tuned to control the electron density in the gated part of the channel, thus allowing the resonant plasma frequency to vary through the frequency of the incoming signal.

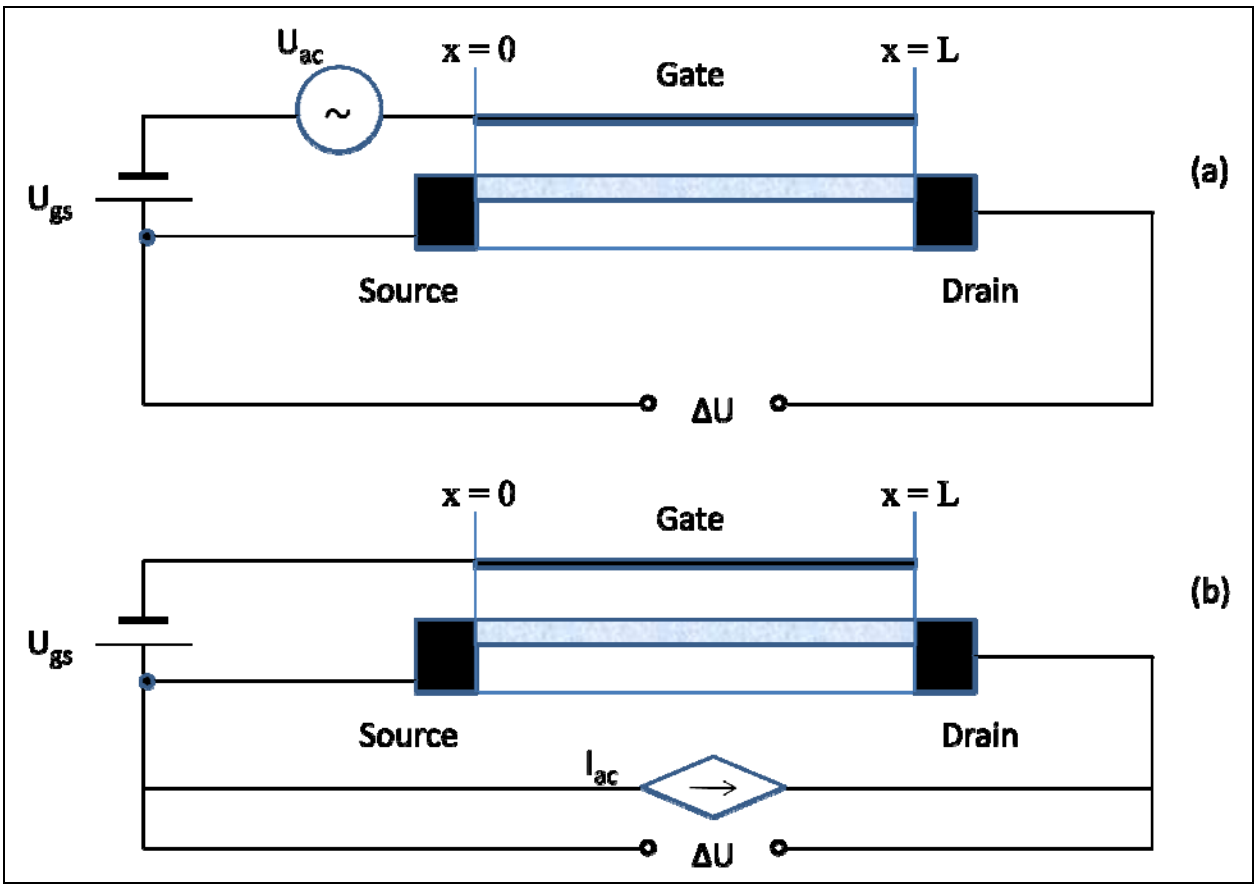

Figure 2. Schematic geometry of FET operating in detector mode for (a) induced ac voltage and (b) induced ac current.

The analysis based on hydrodynamic model of electron gas in the conduction channel (*1*) shows that the detector response ΔU, the constant source-to-drain voltage induced by the incoming ac signal of amplitude U_a and circular frequency ω in the configuration shown in figure 2(a), is given by

$$\frac{\Delta U}{U_0} = \left(\frac{U_a}{U_0}\right)^2 f(\omega), \tag{3}$$

where $U_0=U_g-U_{th}$. In high mobility short channels such that $s\tau_p/L >>1$, the function $f(\omega)$ has a resonant structure. The detector response in the above equation is due to non-linear plasma response in the channel, as will be shown in some detail later in the report. The propagation of the plasma waves in the channel with high density of electrons is much faster than electron drift transport. The non-linear properties of these collective excitations allow the detector's response at frequencies considerably higher than the FET cutoff frequency, determined by the electrons ballistic transport. The width of the resonance is determined by the momentum relaxation rate $1/\tau_p$ that limits the electron mobility, and by the hydrodynamic viscosity in the channel. In the published analysis of the non-linear plasma waves in FET channels the kinematic viscosity coefficient ν at low temperature was assumed to be given by a temperature independent value $\hbar/m$, about 15 cm^2/s for GaAs (*1, 9*).

Below I will derive the hydrodynamic equations from the quasi-classical Boltzmann equation using relaxation time approximation for the collision integrals and obtain the temperature dependence of the hydrodynamic transport coefficients, i.e., viscosity and heat conductivity. These equations will be derived as balance equations starting with a non-equilibrium Fermi-Dirac distribution as a zero order term in the expansion of the distribution function in orders of the Knudsen number, the ratio of the mean free path to the characteristic length of density variations (*11*). The first order corrections to the pressure tensor will be obtained using the electron-electron mean free path, and the viscosity terms will be obtained. The non-linear terms in the hydrodynamic equations lead to non-linear effects in the plasma wave propagation in the channel. In particular, a constant voltage (zero harmonic term) will develop in the plasma response to a time-harmonic perturbation. I will apply a perturbation analysis to the evaluation of this non-linear response, evaluate the response function for different values of mobility and viscosity, and estimate the detector response. It will be shown that at low temperatures in high mobility samples, the viscosity is the main physical mechanism that limits the quality of the plasma resonance. I will include the heat transfer equation in the model and evaluate temperature variations in the conduction channel for relevant values of physical parameters.

3. Quasi-classical Approximation

Let **r** and **p** be 2D position and momentum and **v** is 2D velocity $v = v_F\mathbf{p}/p$. The quasi-classical Boltzmann transport equation for the distribution function $f(\mathbf{r},\mathbf{p},t)$ of electrons in the 2D conduction channel (z = 0) is

$$\frac{\partial f}{\partial t} + \mathbf{v}\cdot\nabla_{\mathbf{r}} f + e\nabla_{\mathbf{r}} U\cdot\nabla_{\mathbf{p}} f = \left(\frac{\partial f}{\partial t}\right)_{ee} + \left(\frac{\partial f}{\partial t}\right)_{R}, \tag{4}$$

where U(**r**,z,t) is the electric potential to be determined self-consistently, e is the charge of electron, the first term on the right hand side is the collision integral due to electron-electron scattering, the second term is the collision integral due to electron-impurity and electron-phonon scatterings. The electron density n(**r**,t) in the channel is obtained from the distribution function as

$$n(\mathbf{r},t) = \frac{g_s}{(2\pi\hbar)^2}\int d^2p f(\mathbf{r},\mathbf{p},t)\,, \tag{5}$$

where g_s =2 is spin degeneracy factor. Electric potential is found from the Poisson equation (in SI units)

$$\nabla_{\mathbf{r}}^2 U + \frac{\partial^2 U}{\partial z^2} = \frac{e}{\varepsilon_s\varepsilon_0}\delta(z)n(\mathbf{r})\,, \tag{6}$$

where ε_s is the value of the background static dielectric constant and $\varepsilon_0 = 8.854\times10^{-12}$ F/m. If the gate contact is at z = d, the boundary condition is a zero tangential field at z =d. In the limit of the infinitely long channel, the Poisson equation can be solved by Fourier transformation,

$$U(\mathbf{q},z) = \int d^2r e^{-i\mathbf{q}\cdot\mathbf{r}} U(\mathbf{r},z) \tag{7}$$

with the result

$$U(\mathbf{q},0) = -\frac{en(\mathbf{q})}{\varepsilon_s\varepsilon_0 q\left[1+\coth(qd)\right]}\,. \tag{8}$$

In the long wave-length limit qd → 0, one obtains the "gradual channel" approximation (*9*) U = en/C, where capacitance per unit area C = $\varepsilon_s\varepsilon_0$/d.

In an equilibrium state with zero drift velocity, f(**r**,**p**,t) is a Fermi-Dirac distribution defined by temperature T and chemical potential ζ. We assume a parabolic conduction band and obtain from the equation $(\partial f/\partial t)_{ee} = 0$ (*11*):

$$f^0(\mathbf{p}) = \left[1+\exp\left(\frac{(\mathbf{p}-m\mathbf{u})^2}{2k_BT} - \xi\right)\right]^{-1} \tag{9}$$

where ξ is the chemical potential ζ divided by temperature, $\xi = \zeta/k_BT$, with the chemical potential determined by the normalization equation 5 with f replaced by f^0:

$$\varsigma = k_BT\ln\left(e^{E_F/k_BT} - 1\right). \tag{10}$$

At low temperature $f^0 \to \theta(p-p_F)$ where p_F is Fermi momentum. We also define Fermi wave vector $k_F = p_F/\hbar$ and Fermi energy $E_F = \zeta(T=0)$. From the normalization at zero temperature, $k_F = (2\pi n)^{1/2}$ and

$$E_F = \frac{\pi\hbar^2 n}{m}. \tag{11}$$

It is important to note the applicability of the quasi-classical kinetics, i.e., equation 4 at low temperatutes. The spatial condition is for the wave-length of the applied field to be much larger than the de Broglie wavelength of electrons: $1/k >> \hbar/p_F$, while the momentum spread should be much smaller than the spread of the distribution $f^0(p)$: $\hbar k << T/v_F$ where $v_F = p_F/m$. These conditions and the time domain condition are equivalent to $\hbar k v_F << k_B T$, $\hbar\omega << E_F$. Taking k ~ 1/L, the spatial condition becomes

$$k_B T >> 2E_F/Lk_F \tag{12}$$

As examples consider GaAs and GaN channels with gate to channel distance d = 35 nm. For the GaAs channel $m/m_0 = 0.067$ and $\varepsilon_s = 12.5$. The gate to channel capacitance per unit area $C = 3.16\times10^{-3}$ F/m^2, and electron density $n = U_0C/e$ where $U_0 = U_g - U_{th}$. At $U_0 = 0.5$ V we obtain $n \approx 1\times10^{12}$ 1/cm^2, $E_F \approx 35$ meV, $v_F = 4.32\times10^7$ cm/s. If L = 0.2 μm, equation 12 requires T >> 16 K. For the GaN channel $m/m_0 = 0.2$ and $\varepsilon_s = 8.9$. Then $C = 2.25\times10^{-3}$ F/m^2. At $U_0 = 1$ V we obtain $n \approx 1.4\times10^{12}$ 1/cm^2, $E_F \approx 16.8$ meV, $v_F = 1.72\times10^7$ cm/s. If L = 0.2 μm, equation 12 requires T >> 7 K. Thus the validity of quasi-classical theory for very short channels requires temperatures considerably higher than 10 K. In the terahertz range $f \sim 1$ THz, $\hbar\omega \sim 4$ meV, and the frequency restriction is fulfilled.

Considering linear response to a harmonic electrical field (*11*), we obtain the quasi-classical dielectric function in a two-dimensional gated channel:

$$\varepsilon(q,\omega) = 1 + \alpha K(q)\left\{1 - e^{-E_F/k_BT} + \omega\int_0^\infty dp\left(\frac{\partial f_p^0}{\partial p}\right)\left[\frac{\Theta(\omega - qp/m)}{\sqrt{\omega^2 - (qp/m)^2}} - \frac{\Theta(qp/m - \omega)}{\sqrt{(qp/m)^2 - \omega^2}}\right]\right\} \tag{13}$$

where $\Theta(\omega)$ is the step function,

$$K(q) = \frac{1}{qd\left[1 + \coth(qd)\right]}, \tag{14}$$

$$\alpha = \frac{e^2md}{\pi\varepsilon_0\varepsilon_s\hbar^2}. \tag{15}$$

At temperatures such that $k_BT < E_F/2$, $\exp(-E_F/k_BT)$ is small and the integral in equation 13 can be simplified to obtain an approximation

$$\varepsilon(q,\omega) = 1 + \alpha K(q)\left(1 - e^{-E_F/k_BT}\right)\left\{1 - \frac{\omega\Theta(\omega - qv_0)(1\text{-}G_T)}{\sqrt{\omega^2 - q^2v_0^2}} - \frac{i\Theta(qv_0 - \omega)G_T}{\sqrt{q^2v_0^2 - \omega^2}}\right\} \tag{16}$$

where

$$G_T(q,\omega) = \left[1 - e^{-E_F/k_B T} + e^{\left(\frac{m\omega^2}{2k^2} - E_F\right)/k_B T} \right]^{-1} \tag{17}$$

$$v_0 = v_F \left[1 + \frac{k_B T}{E_F} \ln\left(1 - e^{-E_F/k_B T}\right) \right] \tag{18}$$

The plasmon dispersion is obtained from the equation $\mathrm{Re}\{\varepsilon(k,\omega_{pl})\} = 0$. Then, if the factors of $\exp(-E_F/k_B T)$ are neglected, we obtain

$$\omega_{pl}(k) = \frac{k v_F}{\sqrt{1 - \frac{1}{\left(1 + 1/\alpha K(k)\right)^2}}} \tag{19}$$

In the examples considered above, α is much larger than 1, namely 14.1 and 59.4 for GaAs and GaN channels respectively. For $\alpha >> 1$ and $kd \leq 1$, equation 16 can be replaced by

$$\omega_{pl}(k) \approx k v_F \sqrt{\frac{\alpha}{2} K(k)}\,. \tag{20}$$

In the long wave length limit, $kd << 1$, we obtain the linear dispersion of the equation 1 $\omega_{pl}(k) = sk$ with $s = (eU_0/m)^{1/2}$, where $U_0 = U_g - U_{th}$. It follows from equation 19 that $\omega_{pl} > kv_F$ and $\mathrm{Im}\{\varepsilon(k,\omega_{pl})\} \approx 0$. Therefore, in the quasi-classical approximation the Landau damping (*11*), a resonant transfer of plasma energy to single particle excitations, is small in the gated channel for temperatures below $E_F/2$.

4. Electron-electron Scattering Rate and Mean Free Path in Two-dimensional Gated Channels

The hydrodynamic approximation can be derived from the kinetic equation assuming a sufficiently high electron density, i.e., the mean free path of the electron-electron (e-e) collisions λ_{ee} should be much smaller than the channel length L. In this work I derive the Navier-Stokes equation from the quasi-classical Boltzmann equation (*12, 13*). The hydrodynamic equations can also be derived by statistical averaging of the Heisenberg equations of motion for density and momentum operators (*14*). In this section I evaluate the mean free path defined by electron-electron collisions, which will determine the limits of validity of the hydrodynamic equations. The electron-electron scattering rate will be evaluated from the Fermi Golden Rule as done for the doped channels (*15, 16*), using quasi-classical approximation for the dielectric function.

$$\frac{1}{\tau_{ee}(\mathbf{p},\sigma)} = \frac{2\pi}{\hbar}\sum_{\mathbf{k},\mathbf{q},\sigma'}\left[f^0_{k\sigma'}(1\text{-}f^0_{k\text{-}q,\sigma'})(1-f^0_{p+q,\sigma}) + (1\text{-}f^0_{k\sigma'})f^0_{k\text{-}q,\sigma'}f^0_{p+q,\sigma}\right]\frac{|v(q)|^2}{\left|\varepsilon\left(q,(E_p - E_{p+q})/\hbar\right)\right|} \times \delta\left(E_{p+q} + E_{k-q} - E_p - E_k\right) \tag{21}$$

where index σ refers to electron spin, $E(q) = \hbar^2q^2/2m$, v(q) is the Coulomb interaction in the gated channel:

$$v(q) = \frac{e^2}{\varepsilon_s\varepsilon_0 q\left[1+\coth(qd)\right]}, \tag{22}$$

and the exchange terms where neglected in the interaction matrix element. The inclusion of the exchange terms will increase the scattering rates only by a modest amount (*17*). In terms of the many-body perturbation theory, the first term in the square brackets in equation 21 represents the scattering of quasi-particles and the second term represents the scattering of quasi-holes (defined with respect to the Fermi surface of the electron gas in the conduction band). Summation over **k** and σ in equation 21 produces the imaginary part of susceptibility (*15*) and after converting summation to integration, we obtain

$$\frac{1}{\tau_{ee}(p)} = \frac{e^2}{4\pi^2\hbar^2\varepsilon_s\varepsilon_0}\int_0^\infty dq\frac{1}{1+\coth(qd)}\int_0^\pi d\theta\left[\coth\left(\frac{E_p - E_{p+q}}{2\hbar k_B T}\right) - \tanh\left(\frac{\varsigma - E_{p+q}}{2\hbar k_B T}\right)\right] \times \mathrm{Im}\frac{1}{\varepsilon(q,(E_p - E_{p+q})/\hbar)} \tag{23}$$

where ζ is the chemical potential given in equation 10.

The mean free path for an electron with wave-vector k is obtained as $\lambda(k) = v_k\tau_{ee}(k)$ where $v_k = \hbar k/m$ and τ_{ee} is the inverse of the e-e scattering rate in equation 21. The distribution averaged value of the mean free path, after summing over the spin directions, is defined as

$$\bar{\lambda} = \sum_{\mathbf{p}\sigma} f^0_{p,\sigma}\lambda(p)\frac{1}{\sum_{\mathbf{p}\sigma} f^0_{p,\sigma}} = \frac{1}{\pi n}\int_0^\infty dk k f^0(k)\lambda(k) \tag{24}$$

where p denotes the momentum while k denotes the wave-vector, and $f^0(k)$ is taken at zero drift velocity. The mean free path obtained in this way is shown in figure 3 as a function of temperature, defined in units of the Fermi temperature $T_F = E_F/k_B$, for the GaAs channel. The mean free path for the GaN channel when plotted as function of T/T_F, is similar. It follows from figure 3 that for channel of length L = 0.2 μm, the hydrodynamic approximation for transport can be used for $T/T_F > 0.1$. In our examples the Fermi temperature is 405 K for GaAs and 195 K for GaN channels.

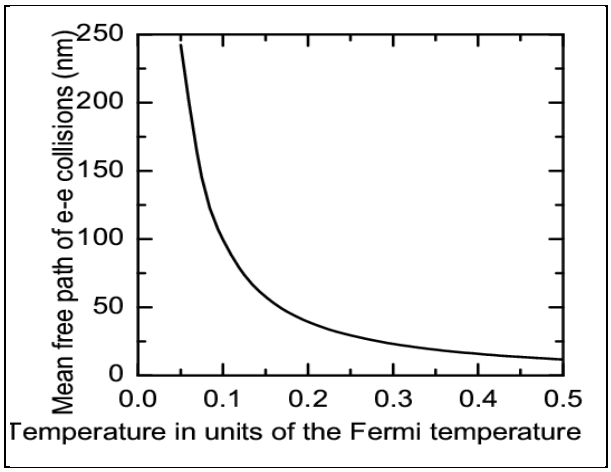

Figure 3. The electron mean free path λ_{ee} determined by the electron-electron scattering is shown as a function of temperature for the GaAs channel, when the gate voltage above the threshold value is $U_0 = 0.5$ V.

5. Derivation of the Hydrodynamic Equations and the Transport Coefficients

The hydrodynamic equations can be derived from the Boltzmann transport equation as balance equations for conserved quantities (*12*). The hydrodynamic variables are plasma density n(**r**,t), given in equation 5, macroscopic velocity **u**(**r**,t), and internal energy ε(**r**,t). The last two are obtained by an ensemble averaging of the corresponding microscopic variables: $\mathbf{u} = \langle \mathbf{v} \rangle$, $\varepsilon = \left\langle m(\mathbf{v}-\mathbf{u})^2/2 \right\rangle$. For a parabolic conduction band assumed here, the microscopic velocity and momentum are linearly related, $\mathbf{v} = \nabla_{\mathbf{p}} E(p) = \mathbf{p}/m$. The collision integral in equation 4 is given by (*11*)

$$\left(\frac{\partial f(\mathbf{p}_1)}{\partial t}\right)_{ee} = \int d\mathbf{p}_2 d\mathbf{p}_3 d\mathbf{p}_4 \{ \; W(\mathbf{p}_3,\mathbf{p}_4,\mathbf{p}_1,\mathbf{p}_2) f(\mathbf{p}_3) f(\mathbf{p}_4)[1-f(\mathbf{p}_1)][1-f(\mathbf{p}_2)] \\ -W(\mathbf{p}_1,\mathbf{p}_2,\mathbf{p}_3,\mathbf{p}_4) f(\mathbf{p}_1) f(\mathbf{p}_2)[1-f(\mathbf{p}_3)][1-f(\mathbf{p}_4)] \; \} \delta(\mathbf{p}_3+\mathbf{p}_4-\mathbf{p}_1-\mathbf{p}_2) , \tag{25}$$

$$W(\mathbf{p}_1,\mathbf{p}_2,\mathbf{p}_3,\mathbf{p}_4) = \frac{2\pi}{\hbar}|M|^2 \delta(E_1+E_2-E_3-E_4) \; ,$$

where M is the Coulomb interaction matrix element. The average of a microscopic variable Q is defined as

$$\bar{Q} \equiv \langle Q \rangle = \frac{\int d^2p \, f(\mathbf{r},\mathbf{p},t) Q}{\int d^2p \, f(\mathbf{r},\mathbf{p},t)} . \tag{26}$$

The balance equations for the density (or charge), momentum, and energy are obtained by setting Q = 1, m**v**, and m(**v**-**u**)^2/2 respectively. The balance equation for the density is obtained in the form of

$$\frac{\partial n}{\partial t} + \nabla \cdot (n\mathbf{u}) = 0 . \tag{27}$$

The electron-electron collision integral does not contribute because of charge, momentum and energy conservation in equation 25 (*12*). For the contribution of the second collision integral in equation 1, I will use the relaxation approximation (*14*), with the relaxation time τ being an inverse of the combined rate of electron-impurity and electro-phonon scatterings. It can be obtained from measured electron mobility in the channel. This gives a friction term in the momentum balance equation:

$$\frac{\partial \mathbf{u}}{\partial t} + (\mathbf{u} \cdot \nabla)\mathbf{u} + \frac{e}{m}\nabla U + \frac{\mathbf{u}}{\tau} = -\frac{1}{n}\nabla \cdot \overleftrightarrow{\Pi} \tag{28}$$

where the pressure tensor was defined:

$$\Pi_{ij} \equiv \left\langle n(v_j - u_j)(v_i - u_i) \right\rangle . \tag{29}$$

The energy balance equation takes the form

$$n\frac{\partial \varepsilon}{\partial t} + n\mathbf{u} \cdot \nabla \varepsilon + \nabla \cdot \mathbf{q} + \Pi_{ij}\Lambda_{ij} = \left(\frac{\partial \varepsilon}{\partial t}\right)_c \tag{30}$$

where **q** is the vector heat flux defined as

$$\mathbf{q} = \frac{mn}{2}\left\langle (\mathbf{v} - \mathbf{u})(\mathbf{v} - \mathbf{u})^2 \right\rangle , \tag{31}$$

the velocity tensor is defined as

$$\Lambda_{ij} = \frac{m}{2}\left(\frac{\partial u_j}{\partial x_i} + \frac{\partial u_i}{\partial x_j}\right), \tag{32}$$

and the internal energy collision integral $(\partial\varepsilon/\partial t)_c$ is related to the energy collision integral $(\partial W/\partial t)_c$ where the energy $W = \varepsilon + mu^2/2$:

$$\left(\frac{\partial \varepsilon}{\partial t}\right)_c = \left(\frac{\partial W}{\partial t}\right)_c - \frac{mu^2}{\tau} . \tag{33}$$

The zero-order approximation to the balance equations is obtained by replacing the distribution function f by its equilibrium form in equation 9 where the density, drift velocity and temperature are functions of position and time. To this order we obtain the energy in terms of temperature and density:

$$\varepsilon = \frac{k_B T F_1(\xi)}{F_0(\xi)}, \tag{34}$$

where the Fermi integrals F_m are defined as

$$F_m(y) = \int_0^\infty dx \frac{x^m}{1+\exp(x-y)}. \tag{35}$$

In the zero-order approximation the heat flux vanishes, $\mathbf{q}^{(0)} = 0$, while the pressure tensor is diagonal, $\Pi^{(0)}_{ij} = \delta_{ij}P$, where the scalar pressure is given by

$$P = \frac{n\varepsilon}{m} = \frac{n k_B T F_1(\xi)}{F_0(\xi)}. \tag{36}$$

In this order the momentum balance equation gives the hydrodynamic Euler equation (*18*). Together with the density balance equation, it was used to predict the nonlinear response of FET to the harmonic perturbation (*1, 2, 9*). The energy balance equation can be put in form of equation for electron temperature. Then, use the energy units and define $\theta(\mathbf{r},t) \equiv k_B T(\mathbf{r},t)$. Define the heat capacity as $c_v \equiv (\partial\varepsilon/\partial\theta)_n = (\partial\varepsilon/\partial T)_n/k_B$ and evaluate it as the heat capacity of the two-dimensional ideal Fermi gas:

$$c_v = \frac{2\theta F_1(\xi)}{E_F} - \frac{E_F}{\theta\left(1-e^{-E_F/\theta}\right)} \tag{37}$$

where E_F is a function of n, see equation 11. Now, writing

$$\nabla\varepsilon = \left(\frac{\partial\varepsilon}{\partial n}\right)_\theta \nabla n + \left(\frac{\partial\varepsilon}{\partial\theta}\right)_n \nabla\theta$$

and using equations 27 and 34 I obtain the equation for the electron temperature distribution. Thus, to zero-order we obtain the Euler equation and the temperature distribution equation:

$$\frac{\partial\mathbf{u}}{\partial t} + (\mathbf{u}\cdot\nabla)\mathbf{u} + \frac{e}{m}\nabla U + \frac{1}{n}\nabla P + \frac{\mathbf{u}}{\tau} = 0 \tag{38}$$

$$\frac{\partial\theta}{\partial t} + \nabla\cdot(\theta\mathbf{u}) = \frac{1}{c_v}\left(\frac{\partial W}{\partial t}\right)_c - \frac{mu^2}{c_v\tau}. \tag{39}$$

From equations 10 and 36 the hydrostatic pressure can be obtained as

$$P = \frac{\theta^2 F_1(\xi)}{\pi\hbar^2}. \tag{40}$$

The effects of viscosity and thermal conductivity appear in the next order of expansion in Knudsen number (*12*). Correspondingly, write the distribution function as

$$f(\mathbf{r},\mathbf{v},t) = f^0(\mathbf{r},\mathbf{v},t) + f^{(1)}(\mathbf{r},\mathbf{v},t) \tag{41}$$

A systematic expansion of the classical distribution function for a parabolic band exists in the form of the Chapman-Enskog expansion (*12*). Here I will use a relaxation time approximation for the first order correction:

$$\left(\frac{\partial f}{\partial t}\right)_{ee} \approx -\frac{f^{(1)}}{\tau_{ee}}. \tag{42}$$

Then, from the Boltzmann equation with only the electron-electron scattering included, one obtains to this order

$$f^{(1)} = -\tau_{ee}\left(\frac{\partial f^0}{\partial t} + v\cdot\nabla_r f^0 + e\nabla_r U\cdot\nabla_p f^0\right) \tag{43}$$

with $f^0 = f^0(n(\mathbf{r},t),\mathbf{u}(\mathbf{r},t),\theta(\mathbf{r},t))$, where n($\mathbf{r}$,t) and $\mathbf{u}$($\mathbf{r}$,t) are solutions of the zero order hydrodynamic equations. Without the relaxation time approximation, one has to solve the linearized Boltzmann equation in order to obtain the transport coefficients in the first order of the expansion in Knudsen number (*11*). In case of fermions in ungated two-dimensional channel, an analytical solution is possible in the low temperature limit (*19*). A much simpler approximation in equation 42 allows one to obtain an estimate of the hydrodynamic transport coefficients in the wider temperature range while giving the correct temperature dependence. The derivation is outlined below. After taking the partial derivatives, the first order contributions are evaluated at $\mathbf{u} = 0$ and we obtain

$$f^{(1)} = -\tau_{ee}(p)\left[f^0\left(1-f^0\right)\right]_{u=0}\left[\left(\frac{m}{2\theta^2}w^2 - \frac{2F_l}{E_F}\right)\mathbf{w}\cdot\nabla\theta + \frac{1}{\theta}\left(w_i w_j - \frac{1}{2}\delta_{ij}w^2\right)\Lambda_{ij}\right] \tag{44}$$

where $\mathbf{w} \equiv \mathbf{v} - \mathbf{u}$. Using this in the evaluation of the ensemble averages in equations 29 and 31, one obtains the pressure tensor and the heat flow to the first order. The pressure tensor can be written as a sum of a unit tensor and a traceless symmetric tensor (*18*), $\Pi_{ij} = \delta_{ij}P + \Pi^{(1)}_{ij}$. Let us define the following integrals over the momentum dependent relaxation time:

$$J_m(T) = \frac{E_F}{\hbar k_F^{m+1}}\int_0^\infty dk k^m \tau_{ee}(k) f^0(k)\left[1-f^0(k)\right] \tag{45}$$

and obtain the first order term in the pressure tensor in the form

$$\Pi^{(1)}_{ij} = -\frac{2\nu n}{m}\left(\Lambda_{ij} - \frac{m}{2}\delta_{ij}\nabla\cdot\mathbf{u}\right) \tag{46}$$

where the kinematic viscosity coefficient ν is given by

$$\nu = \frac{\hbar}{m}\frac{T_F}{T} J_5(T) . \tag{47}$$

Notice that the second viscosity (*18*) does not appear in the pressure tensor in this order, as also is the case in the classical statistics with a parabolic energy band (*11*).

The heat flow is obtained from equations 31 and 44, and to the first order it is proportional to the temperature gradient, as also is the case in the classical fluid:

$$\mathbf{q} = -\kappa\nabla\theta , \tag{48}$$

where the coefficient of thermal conductivity κ is given by

$$\frac{\kappa}{n} = \frac{2\hbar}{m}\left(\frac{J_7 T_F^2}{T^2} - 2F_1 J_5\right). \tag{49}$$

Using equations 46 and 48, one obtains the equations of the viscous hydrodynamic model for the electron fluid in the gated channel as the two-dimensional density balance equation, the Navier-Stokes equation, and the heat equation. Omitting the gradients of the transport coefficients, the equations are:

$$\frac{\partial n}{\partial t} + \nabla\cdot(n\mathbf{u}) = 0 \tag{50}$$

$$\frac{\partial \mathbf{u}}{\partial t} + (\mathbf{u}\cdot\nabla)\mathbf{u} + \frac{e}{m}\nabla U + \frac{1}{n}\nabla P + \frac{\mathbf{u}}{\tau} - \nu\nabla^2\mathbf{u} = 0 \tag{51}$$

$$\frac{\partial\theta}{\partial t} + \nabla\cdot(\theta\mathbf{u}) - \frac{\chi}{c_v}\nabla^2\theta - \frac{m\nu}{2c_v}\left(\frac{\partial u_i}{\partial x_j} + \frac{\partial u_j}{\partial x_i} - \delta_{ij}\frac{\partial u_k}{\partial x_k}\right)^2 = \frac{1}{c_v}\left(\frac{\partial W}{\partial t}\right)_c - \frac{mu^2}{c_v\tau} , \tag{52}$$

where we defined the coefficient $\chi \equiv \kappa/n$, which has the same units as kinematic viscosity. This coefficient divided by the heat capacity, χ/c_v, is the thermometric conductivity (*18*). The coefficients of viscosity and thermal conductivity for GaAs and GaN channels are shown in figure 4 as functions of temperature, T/T_F.

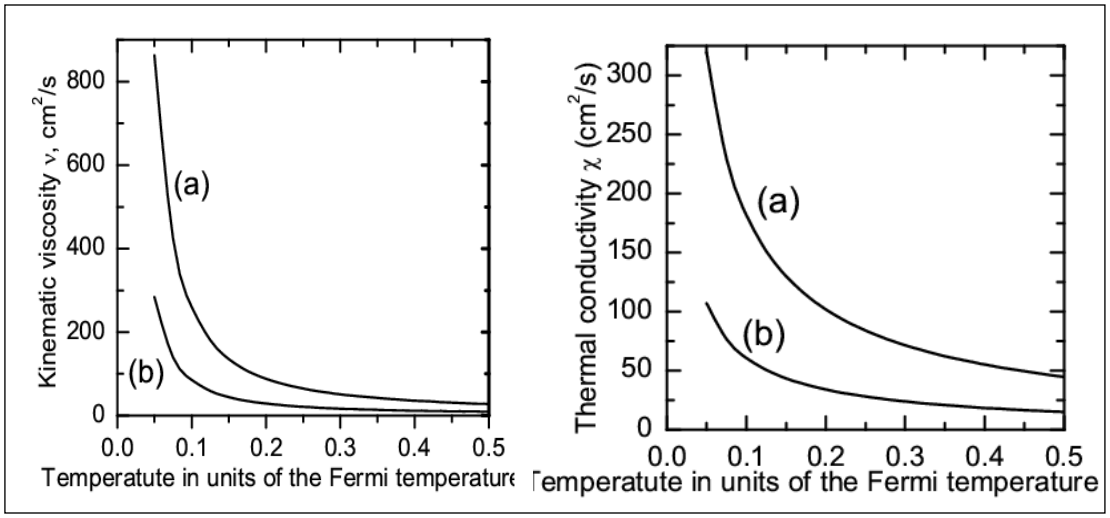

Figure 4. Coefficients of kinematic viscosity (left panel) and thermal conductivity divided by density (right panel) are shown as functions of temperature for the (a) GaAs and (b) GaN channels.

In the low temperature limit the electron-electron collision time $\tau_{ee}(p)$ in equation 45 can be replaced by its value at the Fermi surface, $\tau_{ee}(p_F)$ (*15, 16*) and an explicit temperature dependence can be obtained for the transport coefficients:

$$\nu(T << T_F) \approx \frac{2\hbar}{\pi m}\frac{T_F^2}{T^2}\frac{1}{\ln\left(2T_F/T\right)} \tag{53}$$

$$\frac{\kappa(T << T_F)}{n} \approx \frac{4\pi\hbar}{3m}\frac{T_F}{T}\frac{1}{\ln\left(2T_F/T\right)}. \tag{54}$$

Notice that the temperature dependence is same as one would obtain without the relaxation time approximation by solution of the linearized Boltzmann equation (*19*).

It is clear from figure 4 and equation 53 that at moderately low temperatures the viscosity can be much larger than the value assumed in the published studies of FET based plasma resonator, a constant equal ħ/m (*1–9*). As shown below, at the temperatures at which many of the experimental studies of Dyakonov-Shur detector were performed (*3–7, 10*) the viscosity can be a major limiting mechanism for the quality of the plasma resonance.

In order to compare the relative contributions of the self-consistent field and the pressure gradient terms in the Navier-Stokes equation 51, assume a uniform flow and use the gradual channel approximation, U= en/C, and then obtain:

$$\frac{(1/n)\nabla P}{(e/m)\nabla U} \approx \frac{\pi\hbar^2 C}{me^2}\left[1+\frac{k_B T}{E_F}\frac{F_1}{F_0}-\frac{F_1}{\left(1-e^{-\xi}\right)F_0}\right]. \tag{55}$$

This ratio generally will be small if $T < T_F$. Consider for example a GaAs channel, d = 35 nm, at $U_g - U_{th} = 1$ V. Then the low temperature limit of the right hand side in equation 55 is 0.075. The

linear approximation to the hydrodynamic equations has solutions in the form of plasma waves propagating with the speed $s_{pl} = \sqrt{s_0^{\,2} + s_a^{\,2}}$, where s_0 is obtained from the electric field term in the momentum balance equation and is given in equation 20, and s_a is the speed of sound obtained from the pressure gradient term. At the electron density in the channel with gate voltages of 0.5 ÷ 10 V, $s_a^2 << s_0^2$, one can neglect the pressure gradient term compared to the electric field term (*20*).

The relaxation time τ in the friction term in equation 50 can be related to the mobility η in the channel, $\eta = e\tau/m$. For the collision term in equation 52, $(\partial W/\partial t)_c$, I will use a relaxation approximation (*13*), $(\theta - \theta_0)/\tau_\varepsilon$ where θ_0 is the lattice temperature, and the energy relaxation time τ_ε can be calculated from the electron-phonon scattering rate (*14*).

6. Nonlinear Response of the Channel Confined Electron Plasma to a Time-harmonic Signal

As a simple application of the hydrodynamic equations in this section, I will calculate the response function of the Dyakonov-Shur detector based on the FET conduction channel using the equivalent circuit in figure 2(a). In doing this, I will generalize the treatment in reference 1 to include the effects of viscosity, and also evaluate the electron temperature distribution in the channel. The boundary conditions are $U(0,t) = U_0 + U_a\cos(\omega t)$ at the source side of the channel and zero current at the drain side, $j(L,t) = 0$. In the detector mode, the time-harmonic part is induced by the external radiation (*1–7*). Here the analysis is restricted to a one-dimensional flow that is uniform in the transverse channel direction:

$$\frac{\partial n}{\partial t} + \frac{\partial (nu)}{\partial x} = 0 \tag{56}$$

$$\frac{\partial u}{\partial t} + u\frac{\partial u}{\partial x} + \frac{e}{m}\frac{\partial U}{\partial x} + \frac{1}{n}\frac{\partial P}{\partial x} + \frac{u}{\tau} - \nu\frac{\partial^2 u}{\partial x^2} = 0 \tag{57}$$

$$\frac{\partial \theta}{\partial t} + \frac{\partial (\theta u)}{\partial x} - \frac{\chi}{c_v}\frac{\partial^2 \theta}{\partial x^2} - \frac{m\nu}{c_v}\left(\frac{\partial u}{\partial x}\right)^2 = \frac{1}{c_v}\left(\frac{\partial W}{\partial t}\right)_c - \frac{mu^2}{c_v\tau} \tag{58}$$

In the narrow channel, approximation $n = CU/e$. Then, the boundary condition at the source contact becomes $n(0,t) = n_0 + n_a\cos(\omega t)$. As agued above, the pressure gradient term in equation 57 can be omitted as compared to the electric field term. Then, if one assumes that the temperature variation is small enough to ignore the space-time variation of the viscosity, the Navier-Stokes equation effectively decouples from the heat equation, equation 58.

For convenience use dimensionless variables and parameters, defined as

$$\tilde{t} = ts_0/L,\ \tilde{x} = x/L,\ \tilde{n} = n/n_0, \tilde{u} = u/s_0, \tilde{\tau} = \tau s_0/L, \tilde{\nu} = \nu/(s_0 L),\ \ \tilde{\chi} = \chi/Ls_0,\ \tilde{\theta} = \theta/ms_0^{\ 2} \tag{59}$$

where s_0 is the equilibrium value of the plasma wave velocity. The hydrodynamic equations derived in the previous section can be written in the dimensionless form,

$$\frac{\partial \tilde{n}}{\partial \tilde{t}} + \frac{\partial(\tilde{n}\tilde{v})}{\partial \tilde{x}} = 0, \tag{60}$$

$$\frac{\partial \tilde{u}}{\partial \tilde{t}} + \tilde{u}\frac{\partial \tilde{u}}{\partial \tilde{x}} + \frac{\partial \tilde{n}}{\partial \tilde{x}} + \frac{\tilde{u}}{\tilde{\tau}} - \tilde{\nu}\frac{\partial^2 \tilde{u}}{\partial \tilde{x}^2} = 0, \tag{61}$$

$$\frac{\partial \tilde{\theta}}{\partial \tilde{t}} + \frac{\partial(\tilde{\theta}\tilde{u})}{\partial \tilde{x}} - \frac{\tilde{\chi}}{c_v}\frac{\partial^2 \tilde{\theta}}{\partial \tilde{x}^2} - \tilde{\nu}\left(\frac{\partial \tilde{u}}{\partial \tilde{x}}\right)^2 + \frac{\theta - \theta_0}{\tilde{\tau}_\theta} + \frac{\tilde{u}^2}{c_v \tilde{\tau}} = 0 \tag{62}$$

where we defined $\tau_\theta \equiv c_v \tau_\varepsilon$. When the solution u(x,t) of the equations 60 and 61 is found, it can be used in equation 62 to obtain an inhomogeneous heat equation which then can be solved to obtain the electron temperature distribution θ(x,t) in the channel.

The boundary conditions are

$$\tilde{n}(0,t) = 1 + \tilde{n}_a \cos(\omega t),\ \tilde{u}(1,t) = 0. \tag{63}$$

Expand the solutions of equations 59 and 60 in time harmonics:

$$\tilde{n} - 1 = n^{(0)} + n^{(1)} + n^{(2)} + \ldots \tag{64}$$

$$\tilde{u} = u^{(0)} + u^{(1)} + u^{(2)} + \ldots \tag{65}$$

where $n^{(m)}, v^{(m)} \propto \exp(im\omega t)$, m=0,1,2…. The hydrodynamic nonlinearities result in coupling of different harmonics. Assuming that the input signal is small, $\tilde{n}_a << 1$ and $\tilde{u} << 1$, apply the small signal analysis. This obtains the following hierarchy of orders of expansion:

$$n^{(1)}, u^{(1)} = O(\tilde{n}_a);\ n^{(2)}, n^{(0)} = O(\tilde{n}_a^2);\ u^{(0)}, u^{(2)} = O(\tilde{n}_a^2). \tag{66}$$

Separating the orders and integrating over the time in the second order equations, obtain

$$\frac{\partial n^{(1)}}{\partial \tilde{t}} + \frac{\partial u^{(1)}}{\partial \tilde{x}} = 0 \tag{67}$$

$$\frac{\partial u^{(1)}}{\partial \tilde{t}} + \frac{\partial n^{(1)}}{\partial \tilde{x}} + \frac{u^{(1)}}{\tilde{\tau}} - \tilde{\nu}\frac{\partial^2 u^{(1)}}{\partial \tilde{x}^2} = 0 \tag{68}$$

$$\frac{\partial}{\partial \tilde{x}}\left(u^{(0)} + \left\langle n^{(1)} u^{(1)} \right\rangle\right) = 0 \tag{69}$$

$$\frac{\partial}{\partial \tilde{x}}\left(\frac{1}{2}\left\langle u^{(1)2}\right\rangle + n^{(0)}\right) + \frac{2u^{(0)} + \left\langle n^{(1)}u^{(1)}\right\rangle}{\tilde{\tau}} - \tilde{\nu}\frac{\partial^2 u^{(0)}}{\partial \tilde{x}^2} = 0 \tag{70}$$

where the angular brackets denote time average over the period $2\pi/\omega$. Boundary conditions for these equations are

$$n^{(1)}(0,\tilde{t}) = \tilde{n}_a \cos(\omega t),\ n^{(0)}(\tilde{x}=0) = u^{(0)}(\tilde{x}=1) = u^{(1)}(1,\tilde{t}) = 0.$$

The induced constant source to drain voltage will be found as

$$\Delta U = (e/C))n_0 \Delta\tilde{n}^{(0)} \equiv (e/C))n_0\left[\tilde{n}^{(0)}(\tilde{x}=1) - \tilde{n}^{(0)}(\tilde{x}=0)\right] \tag{71}$$

From equations 69 and 70, obtain

$$\Delta\tilde{n}^{(0)} = \frac{1}{2}\left\langle u^{(1)2}(0)\right\rangle + \frac{1}{\tilde{\tau}}\int_0^1 d\tilde{x}\left\langle n^{(1)}u^{(1)}\right\rangle - \tilde{\nu}\left\langle n^{(1)}(0)u^{(1)}(0)\right\rangle \tag{72}$$

where the arguments refer to x. The first order functions $n^{(1)}$ and $u^{(1)}$ are solutions of equations 67 and 68 which give linear wave equation, with solutions proportional to $\exp(ikx-i\omega t)$. The dispersion relation is

$$\omega^2 + i\omega/\tau - k^2\left(s_0{}^2 - i\nu\omega\right) = 0\,. \tag{73}$$

The solutions of equations 67 and 68 are

$$n^{(1)} = \mathrm{Re}\left\{\left(\tilde{C}_1 e^{ik_0x} + \tilde{C}_2 e^{-ik_0x}\right)e^{-i\omega t}\right\} \tag{74}$$

$$u^{(1)} = \mathrm{Re}\left\{\left(\tilde{C}_1 e^{ik_0x} - \tilde{C}_2 e^{-ik_0x}\right)e^{-i\omega t}\right\} \tag{75}$$

where $k_0(\omega)=k_1 + ik_2$ is solution of equation 73 and

$$k_{1,2} = \frac{\omega}{s_0{}^2\sqrt{1+\omega^2\tau_1{}^2}}\frac{1}{\sqrt{2}}\left\{\pm\left(1-\frac{\tau_1}{\tau}\right) + \left[\left(1-\frac{\tau_1}{\tau}\right)^2 + \left(\frac{1}{\omega\tau} + \omega\tau_1\right)^2\right]^{1/2}\right\}^{1/2}. \tag{76}$$

Here I defined $\tau_1 = \nu/s_0{}^2$. Constants C_1 and C_2 are found from the boundary conditions:

$$\tilde{C}_{1,2} = \frac{\tilde{n}_a}{1+\exp\left(\pm 2ik_0L\right)}\,. \tag{77}$$

Then use equations 74 and 75 in equation 72, and use equation 71 to find constant source to drain voltage ΔU induced by the harmonic input signal. This can be written as in equation 3:

$$\frac{\Delta U}{U_0} = \left(\frac{U_a}{U_0}\right)^2 f(\omega),$$

where the detector response function f(ω) is given in terms of $k_0(\omega)$. Let us define the following combinations of hyperbolic and trigonometric functions of k_1L and k_2L:

$$S_1 = \cosh(2k_2L) - \cos(2k_1L)$$

$$S_2 = \frac{k_1}{k_2}\left[\cosh(2k_2L) - 1\right] + \frac{k_2}{k_1}\left[1 - \cos(2k_1L)\right]$$

$$S_3 = k_1 \cosh(2k_2L) + k_2 \cos(2k_1L)$$

$$S_4 = \cosh(2k_2L) + \cos(2k_1L).$$

In terms of these the detector response function is given by

$$f(\omega) = \left[\frac{(\omega\tau)^2 S_1}{\tilde{\tau}^2} + \frac{\omega\tau S_2}{2\tilde{\tau}^2} - \frac{2\tilde{\nu}\omega\tau S_3}{\tilde{\tau}}\right]\frac{1}{|k_0L|^2 S_4}, \tag{78}$$

where $\tilde{\nu}$ and $\tilde{\tau}$ are defined in equation 59. Depending on the value of the friction parameter $\hat{\imath}$, the detector response will be resonant or broadband.

Next, consider the behavior of the response function in the case of the GaAs channel of length L = 0.5 μm, gate insulator thickness d = 35 nm, and set U_0 = 0.5 V as in the first example in section III. The temperature dependence of the friction parameter at low to moderate temperatures is determined by the electron-acoustic phonon scattering rate, and the total rate is given by

$$\frac{1}{\tau} = \frac{1}{\tau_0} + aT \tag{79}$$

where the zero temperature value $1/\tau_0$ is due to scattering from impurities and defects. We set here τ_0 = 10 ps (the corresponding low temperature mobility is about 2.7×10^5 cm^2/Vs). For GaAs heterostructure we obtain (*21, 22*) a = 7.1×10^8 1/Ks. This determines the friction parameter $\hat{\imath}$ as a function of temperature, while the temperature dependence of the viscosity coefficient is found from equation 47 and figure 4. The resonant frequency $f_0 = \omega_0/2\pi = s_0/4L$ = 0.57 THz. In figure 5 the resonant response is shown at two values of T/T_F, 0.1 and 0.15, corresponding to T = 40.6 K and 60.9 K. The corresponding values of the friction parameter $s_0\tau/L$ are 17.7 and 15.9 and of the kinematic viscosity coefficient 260 and 135 cm^2/s. The higher resonances are strongly diminished by the viscosity effect.

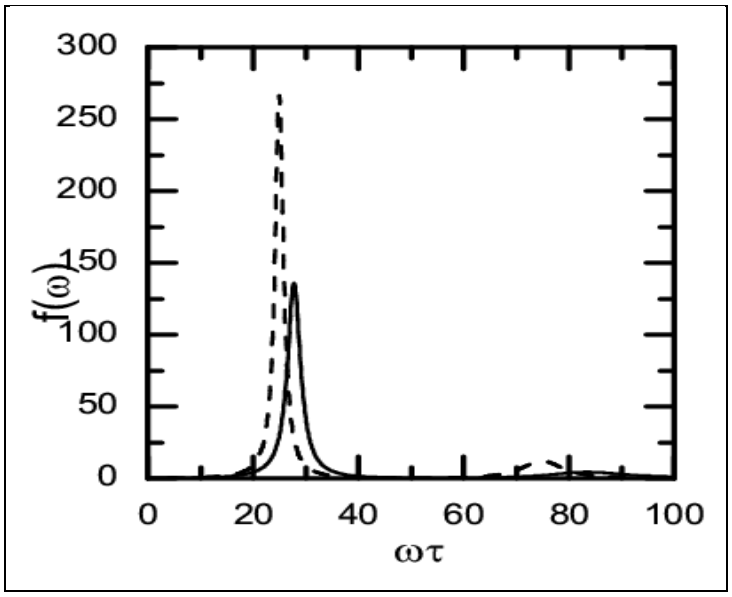

Figure 5. Response function of the GaAs channel based detector at two different temperatures: $T/T_F = 0.1$ (solid line) and $T/T_F = 0.15$ (broken line).

When the friction parameter $\tau s_0/L$ decreases below 0.5, the response becomes broadband, corresponding to overdamped plasma oscillations in the conduction channel, as shown in figure 6 for $\tau s_0/L = 0.3$ and 0.2 with $\nu/s_0L = 0.001$. For a long channel, as $\tau s_0/L$ decreases the plasma waves decay before ever reaching the drain contact.

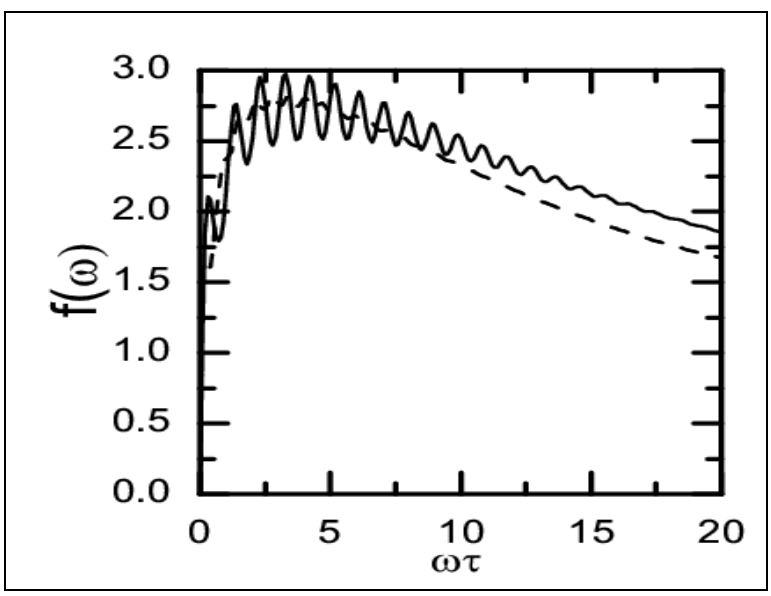

Figure 6. Response function in the case of strongly damped plasma oscillations, giving a broadband detector response, for two different values of friction parameter, $\tau s_0/L = 0.3$ and 0.2 with $\nu/s_0L = 0.001$.

Next, turn to the evaluation of the electron temperature distribution in the channel to $O(n_a)$. To that order the u^2 and $(\partial u/\partial x)^2$ terms in equation 62 can be omitted. Define $\Delta\theta \equiv \theta - \theta_0$ and

$$\Phi(\tilde{x},\tilde{t}) = -\tilde{\theta}_0 \frac{\partial \tilde{u}}{\partial \tilde{x}} \tag{80}$$

where θ_0 refers to lattice temperature and u(x,t) is given in equation 74. Then obtain an equation for $\Delta\theta$:

$$\frac{\partial \Delta\tilde{\theta}}{\partial \tilde{t}} = \tilde{\chi}' \frac{\partial^2 \Delta\tilde{\theta}}{\partial \tilde{x}^2} - \frac{\Delta\tilde{\theta}}{\tilde{\tau}_\theta} + \Phi(\tilde{x},\tilde{t}) \tag{81}$$

where $\chi' \equiv \chi/c_v$. For the boundary conditions, assume lattice temperature at the source and drain contacts and assume that the electron temperature was initially set to the lattice value:

$$\Delta\theta(0,\tilde{t}) = \Delta\theta(1,\tilde{t}) = 0, \quad \Delta\theta(\tilde{x},0) = 0\,. \tag{82}$$

Substitution $\Delta\theta(x,t) = f(x,t)\exp\left(-t/\tau_\theta\right)$ transforms equation 80 into

$$\frac{\partial f}{\partial \tilde{t}} = \tilde{\chi}' \frac{\partial^2 f}{\partial \tilde{x}^2} + \Phi(\tilde{x},\tilde{t})\exp\left(-\tilde{t}/\tilde{\tau}_\theta\right), \tag{83}$$

which is the inhomogeneous heat equation with Dirichlet boundary conditions (*23*). The Green's function for this equation can be evaluated by Fourier expansion in the interval $0 \le x \le 1$, and restoring the dimensional units we obtain

$$\frac{\Delta T}{T_0} = -2\frac{n_a}{n_0} Re \sum_{m=1}^{\infty} \left\{ \left[\exp\left(-i\omega t\right) - \exp(-a_m t)\right] \frac{k_0 L \pi m \sin\left(\pi m x/L\right)\left[1 + (-1)^{m-1}\sec(k_0 L)\right]}{\left(\omega L/s_0 + i a_m\right)\left(\pi^2 m^2 - k_0^2 L^2\right)} \right\} \tag{84}$$

where $a_m = \dfrac{\pi^2 m^2 \chi'}{L s_0} + \dfrac{L}{s_0 \tau_\theta}$.

As an example, consider a signal with the amplitude equal to 0.1 of the gate voltage applied to a GaAs channel with $s_0\tau/L = 2$ (corresponding to mobility of 54000 cm^2/Vs), and we set $s_0\tau_\theta/L = 2$, $\nu/s_0L = 0.04$, $\chi/(c_v s_0 L) = 0.16$. The deviation of the electron temperature T(x,t) from the lattice temperature T_0 is shown in figure 7 as a function of the position along the channel at times $ts_0/L = 1$ and 2, evaluated at the resonance frequency.

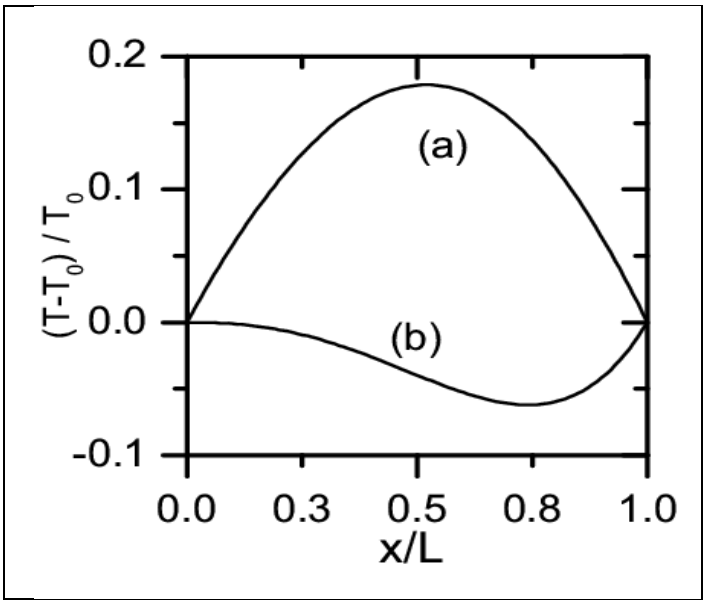

Figure 7. An example of electron temperature distribution in the conduction channel with $s_0\tau/L = 2$, at two different times (a) $ts_0/L = 1$ and (b) $ts_0/L = 2$. Both distributions are evaluated at the resonance frequency ω_0, with the amplitude of the applied signal equal to $0.1U_0$.

As another example, consider the case corresponding to the solid line in figure 5, i.e., GaAs channel at lattice temperature $T = 0.1T_F$, when the signal of amplitude $0.01U_0$ and $\omega = \omega_0$ is applied. The resulting temperature distribution is shown in figure 8, at two times, (a) $ts_0/L = 1$ and (b) $ts_0/L = 2$.

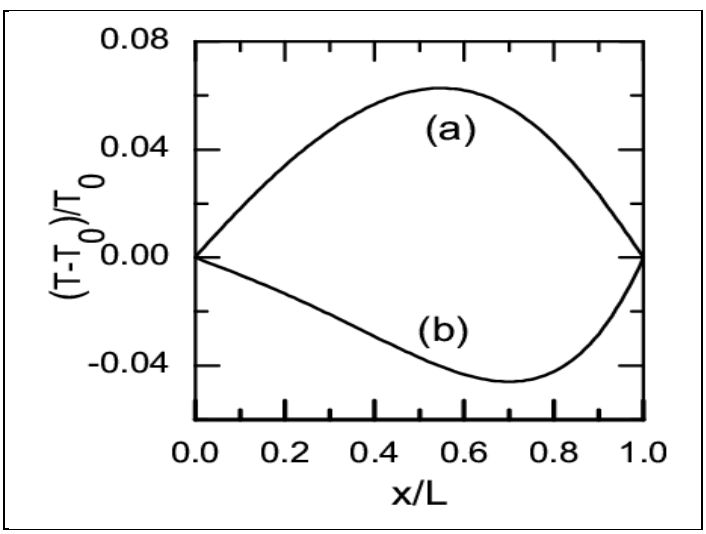

Figure 8. Electron temperature distribution in the GaAs conduction channel at $T_0 = 0.1T_F$ at two different times, (a) $ts_0/L = 1$ and (b) $ts_0/L = 2$ in. Both distributions are evaluated at the resonance frequency ω_0, with the amplitude of the applied signal equal to $0.01U_0$.

Note that in these examples the variation of the electron temperature in the channel is relatively small when the applied signal is small. This justifies the approximation of uniform electron temperature in the solution of the Navier-Stokes equation. At much higher mobility and when the applied signal is not small as compared to the gate voltage, the temperature dependence of the transport coefficients may have to be included explicitly in equations 60–62 which then would have to be solved numerically.

One can estimate the sensitivity of the detector following reference 1. If the electro-magnetic radiation is coupled to device by means of dipole antenna, the detector response is given by $R = \Delta U/(IS)$, where I is the radiation energy density in the incoming signal, ΔU is given in equation 3, and the antenna aperture $S = \lambda^2 G/4\pi$. Here λ is the wavelength and $G \approx 1.5$ is the antenna gain. We then obtain an estimate $R \sim (100/U_0)f(\omega)$ V/W. For the example shown in figure 5, $R \sim 10^4$ V/W.

The predicted response is smaller than was originally predicted for semiconductor HEMT device at low temperature (*1*), due to significant increase of viscosity coefficient with the decreasing temperature. Most experiments with the Dyakonov-Shur plasma resonators have been done at low temperature in order to reduce electron-phonon scattering rate $1/\tau$ and achieve correspondingly high value of mobility, see references 1–10. It follows from the present calculation that at very low temperatures the entropy production associated with viscosity negates the advantage of increasing carrier mobility with lower temperature. One can see it in considering the quality of the plasma resonance at low temperatures. Near the resonant frequency ω_0 the function $f(\omega)$ is approximately a Lorentzian with the width $\Delta\omega$ determined by the friction and viscosity. Define the quality factor Q of the resonance at $\omega = \omega_0$ as $Q \equiv \omega_0/\Delta\omega$. Then

$$\frac{1}{Q} = \frac{2L}{\pi s_0 \tau} + \frac{2\pi \nu}{s_0 L}. \tag{85}$$

The temperature dependence of ν is given in equation 47 and figure 4, and the temperature dependence of τ at low temperature is given in equation 79. The linear coefficient a in equation 79 can be deduced from the temperature dependence of electron mobility in GaAs (*21, 22*) and GaN (*24*) channels, and we obtain values of 7.1×10^8 1/Ks and 22×10^8 1/Ks, respectively. Then the equation 85 can be rewritten as

$$\frac{1}{Q} = \frac{2L}{\pi s_0 \tau_0} + \frac{2LaT}{\pi s_0} + \frac{2\pi \nu(T)}{s_0 L}. \tag{86}$$

With the same parameters as in figure 4 and $\tau_0 = 10$ ps, the resonator quality factor Q is shown in figure 9 as a function of temperature at low temperatures for GaAs and GaN submicron channels, $L = 0.5\mu m$, with the plasma resonance at approximately 0.5 THz.

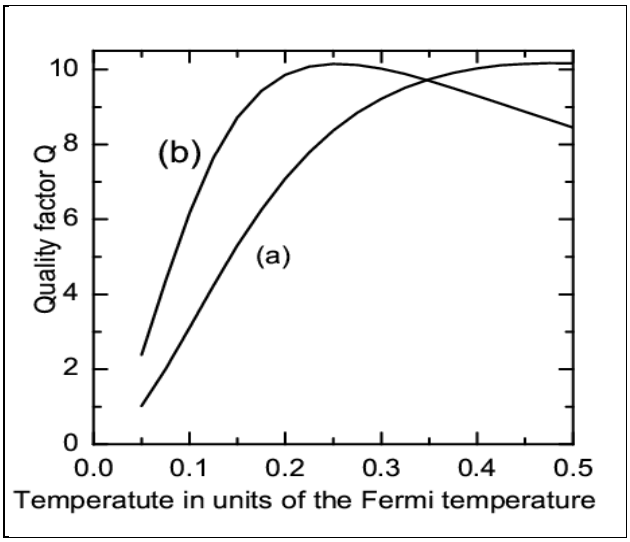

Figure 9. Plasma resonator quality factor is shown as function of temperature for (a) GaAs and (b) GaN channels with length L = 0.5 μm. The resonance is at $f_0 \sim 0.5$ THz.

One can see that the quality factor is limited to values below Q = 10, which agrees with the experimental studies (*4*) in which the loss to transversely propagating waves (oblique plasmons (*25, 26*)) was eliminated by having a multi-channel configuration.

Next, consider resent low temperature experiments (*10*) with the long channel GaAs detector, with L = 180 μm, d = 190 nm, and the measured electron density $n_0 = 1.3\times10^{11}$ 1/cm^2. Correspondingly, the plasma resonance is at $f_0 \approx 1.2$ GHz. By fitting the measured values of mobility as $1/\mu = 1/\mu_0 + \alpha T$ and relating τ to μ by $\tau = m\mu/e$, we find that the scattering rate is obtained from equation 79 with $\tau_0 = 0.539$ ns and $a = 5.45\times10^8$ 1/Ks. The viscosity coefficient can be calculated from equation 53 as

$$\nu(T) \approx 11\left(\mathrm{cm}^2/\mathrm{s}\right)\times\left(\frac{T_F}{T}\right)^2 \frac{1}{\ln\left(2T_F/T\right)}$$

where $T_F = 54$ K. The quality factor evaluated from equation 85 is shown in figure 10 and the results are in reasonable agreement with the resonance widths in reference 10.

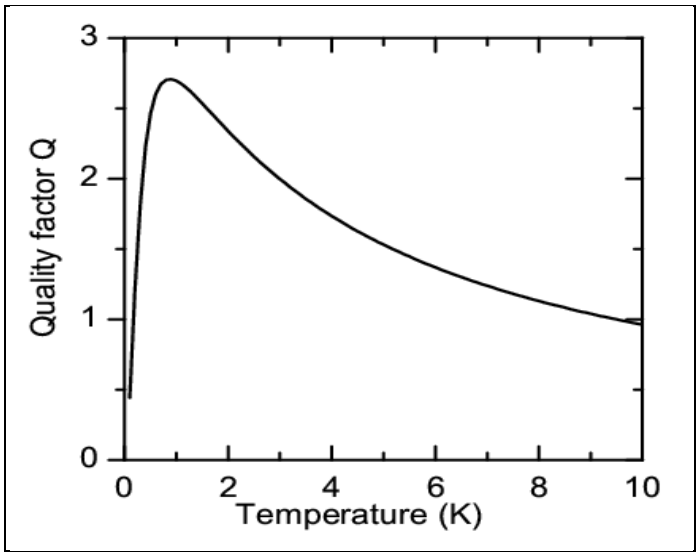

Figure 10. Plasma resonator quality factor is shown as function of temperature for a GaAs detector with channel length L = 180 μm. The resonance is at $f_0 \sim 1.2$ GHz.

Thus, as in the case of short channel plasma resonators discussed above, here too the viscosity effects limit the quality of the resonator at low temperatures, reducing the advantage of higher mobility achieved by lowering the temperature.

7. Conclusions

In this work I considered the non-linear plasma transport in gated conduction channels. The hydrodynamic Navier-Stokes equation was derived from the quasi-classical Boltzmann equation, and the applicability of hydrodynamic model was evaluated. The non-linear convection term in the Navier-Stokes equation and the non-linearity in the current term in the mass balance equation contribute to non-linear effects in the wave propagation in the electron fluid. I evaluated the temperature dependent hydrodynamic transport coefficients in gated two-dimensional conduction channels. I applied these equations to show that a constant voltage develops in the plasma response to a time-harmonic perturbation, and evaluated the response function for different values of mobility and viscosity and we then estimated the detector response. The treatment here extended the theory of Dyakonov-Shur plasma resonator and detector (*1*) to account for the temperature dependence of viscosity, and also included the energy balance equation into the analysis. Depending on the length of the gated channel, the detector response can be in the range from a few GHz to a few THz, and is further tunable by the gate voltage. Depending on electron mobility in the channel the response can be resonant or broadband. I showed that the quality of the plasma resonance in the high mobility channels at low temperature is limited by the effects of viscosity. Though the evaluation of the response was confined to the one-dimensional uniform

flow, the hydrodynamic equations derived here can also be applied to the two-dimensional wave propagation, and the effects of the oblique modes (*26*) can also be included.

8. References

1. Dyakonov, M.; Shur, M. *IEEE Trans. Electron. Devices* **1996**, *43*, 380.
2. Dyakonov, M.; Shur, M. *IEEE Trans. Electron. Devices* **1996**, *43*, 1640.
3. El Fatimi, A.; Teppe, F.; Dyakonova, N.; Knapp, W.; Seliuta, D.; Valusis, G.; Shchepetov, A.; Roelens, Y.; Bollaert, S.; Cappy, A.; Rumyantsev, S. *Appl. Phys. Lett.* **2006**, *89*, 131926.
4. Shchepetov, A.; Gardes, C.; Roelens, Y.; Cappy, A.; Bollaert, S.; Boubanga Tombet, S.; Teppe, F.; Coquillat, D.; Nadar, S.; Dyakonova, N.; Videlier, N.; Knapp, W.; Seliuta, D.; Vadoklis, R.; Valusis, G. *Appl. Phys. Lett.* **2008**, *92*, 242105.
5. El Fatimi, A.; Boubanga Tombet, S.; Teppe, F.; Knapp, W.; Veksler, D. B.; Rumyantsev, S.; Shur, M. S.; Pala, N.; Gaska, R.; Fareed, Q.; Hu, X.; Seliuta, D.; Valusis, G.; Gaquiere, C.; Theron, D.; Cappy, A. *Electronics Lett.* **2006**, *42*, 1342.
6. Gavrilenko, V. I.; Demidov, E. V.; Marem'yanin, K. V.; Morozov, S. V.; Knapp, W.; Lusakowski, J. *Semiconductors* **2007**, *41*, 232.
7. Knapp, W.; Teppe, F.; Dyakonova, N.; Coquillat, D.; Lusakowski, J. *J. Phys. Cond. Matter* **2008**, *20*, 384205.
8. Sizov, F. *Opto-Electron. Review* **2010**, *18*.
9. Dyakonov, M.; Shur, M. *Phys. Rev. Lett.* **1993**, *71*, 2465.
10. Kang, S.; Burke, P.; Pfeiffer, L. N.; West, K. W. *Appl. Phys. Lett.* **2006**, *89*, 213512.
11. Lifshitz, E. M.; Pitaevskii, L. P. Physical Kinetics (Landau Course of Theoretical Physics, v. 10), Butterworth-Heinemann, 1981.
12. Huang, K. *Statistical Mechanics*; John Wiley, 1963.
13. Blotekjer, K. *IEEE Trans. Electron Dev.* **1970**, *ED-17*, 38.
14. Cai, J.; Cui, H. L. *J. Appl. Phys.* **1995**, *78*, 6802.
15. Giuliani, G. F.; Quinn, J. J. *Phys. Rev. B* **1982**, *26*, 4421.
16. Zheng, L.; Das Sarma, S. *Phys. Rev. B* **1996**, *53*, 9964.
17. Qian, Z.; Vignale, G. *Phys. Rev. B* **2005**, *71*, 075112.
18. Landau, L. D.; Lifshitz, E. M. Fluid Mechanics (Landau Course of Theoretical Physics, v. 6), Butterworth-Heinemann, 1987.

19. Lyakhov, A. O.; Mishchenko, E. G. *Phys. Rev. B* **2003**, *67*, 041304(R).

20. Rudin, S.; Samsonidze, G.; Crowne, F. *J. Appl. Phys.* **1999**, *86*, 2083.

21. Walukiewicz, W. *Phys. Rev. B* **1988**, *37*, 8530.

22. English, J. H.; Gossard, A. C.; Stormer, H. L.; Baldwin, K. W. *Appl. Phys. Lett.* **1987**, *50*, 1826.

23. Morse, P. M.; Feshbach, H. *Methods of Theoretical Physics*; McGraw-Hill, 1953.

24. Knapp, W.; Borovitskaya, E.; Shur, M. S.; Hsu, L.; Walukiewicz, W.; Frayssinet, E.; Lorenzini, P.; Grandjean, N.; Skierbiszewski, S.; Prystawko, P.; Leszczynski, M.; Grzegory, I. *Appl. Phys. Lett.* **2002**, *80*, 1228.

25. Popov, V. V. *Appl. Phys. Lett.* **2008**, *93*, 083501.

26. Dyakonov, M. I. *Semiconductors* **2008**, *42*, 984.

No. of Copies	Organization
1 ELECT	ADMNSTR DEFNS TECHL INFO CTR ATTN DTIC OCP 8725 JOHN J KINGMAN RD STE 0944 FT BELVOIR VA 22060-6218
1 CD	OFC OF THE SECY OF DEFNS ATTN ODDRE (R&AT) THE PENTAGON WASHINGTON DC 20301-3080
1	US ARMY RSRCH DEV AND ENGRG CMND ARMAMENT RSRCH DEV & ENGRG CTR ARMAMENT ENGRG & TECHNLGY CTR ATTN AMSRD AAR AEF T J MATTS BLDG 305 ABERDEEN PROVING GROUND MD 21005-5001
1	PM TIMS, PROFILER (MMS-P) AN/TMQ-52 ATTN B GRIFFIES BUILDING 563 FT MONMOUTH NJ 07703
1	US ARMY INFO SYS ENGRG CMND ATTN AMSEL IE TD A RIVERA FT HUACHUCA AZ 85613-5300
1	COMMANDER US ARMY RDECOM ATTN AMSRD AMR W C MCCORKLE 5400 FOWLER RD REDSTONE ARSENAL AL 35898-5000
1	US GOVERNMENT PRINT OFF DEPOSITORY RECEIVING SECTION ATTN MAIL STOP IDAD J TATE 732 NORTH CAPITOL ST NW WASHINGTON DC 20402
1	US ARMY RSRCH LAB ATTN RDRL CIM G T LANDFRIED BLDG 4600 ABERDEEN PROVING GROUND MD 21005-5066

No. of Copies	Organization
8	US ARMY RSRCH LAB ATTN IMNE ALC HRR MAIL & RECORDS MGMT ATTN RDRL CIM L TECHL LIB ATTN RDRL CIM P TECHL PUB ATTN RDRL SER E F CROWN ATTN RDRL SER U C FAZI ATTN RDRL SEE M M WRABACK ATTN RDRL SER A HUNG ATTN RDRL SEE M S RUDIN ADELPHI MD 20783-1197

TOTAL: 16 (1 ELEC, 1 CD, 14 HCS)